System Throughput Analysis on Using Joint Detection in Distributed Antenna System

Haruya Ishikawa, Yukitoshi Sanada
Dept. of Electronics and Electrical Engineering,
Keio University, Yokohama, Japan
Email: haruyaishikawa@snd.elec.keio.ac.jp, sanada@elec.keio.ac.jp

***Abstract*—Throughput analysis of the usage of joint maximum-likelihood detection (MLD) in a distributed antenna system (DAS) with multiple mobile terminal scheduling is evaluated in this paper. In DAS, mobile terminals are closer to desired antennas which improves system throughput and increases frequency utilization efficiency. However, since there are more antennas in a cell, interference can occur between transmitted signals from the antennas when multiple mobile terminals are scheduled. Therefore, we propose a novel mobile terminal scheduling method and the use of joint MLD to reduce the effects of interference. A system level simulation shows that the usage of joint MLD in densely packed DAS provides better system throughput.**

***Index Terms*—Distributed Antenna System, Joint Detection**

I. Introduction

With the on-going popularity of mobile devices such as smartphones and tablet PCs, there are increasing demands for high-speed and large capacity wireless communications [1], [2]. To accommodate for this explosive traffic growth, the fifth generation mobile communication system (5G) is currently being proposed. One solution to improve spectrum efficiency is a distributed antenna system (DAS) [3]. DASs were originally introduced for indoor radio communications simply as a mean to extend coverage to dead spots [4]. However, the DAS's advantages in reducing power consumption and increasing system capacity were quickly exploited to be used in broadband multi-cell environments [5]. In the DAS, several antennas are dispersed in a cell; hence for the name distributed antenna (DA). The DAs are physically connected to a centralized baseband unit (BBU) via highspeed optical fronthaul links [5]. Mobile user terminals (MT) are connected to DAs depending on BBU's configuration such as scheduling criteria. Since low-power DAs are geographically placed throughout the cell to reduce their access distances, the DAS mitigates channel impacts such as shadowing and fading, which deteriorates transmission capacity and coverage [6]. It has been shown that a conventional cell model, such as a centralized antenna system (CAS), does not allow as much, if not any, frequency reuse, resulting in the DAS providing better spectrum efficiency [7].

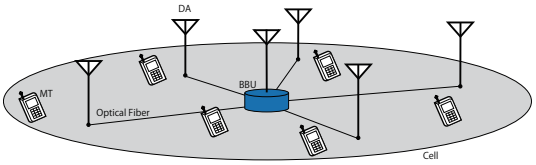

Fig. 1: Distributed antenna system (DAS).

With cell models that deploy multiple antennas near each other, such as the DAS, frequency and channel reuse is a common technique which aims to improve spectral efficiency. However, reusing the same frequency in mobile wireless systems often leads to a degraded link and service quality due to co-channel interference (CCI) occurring at cell coverage boundaries. In order to suppress interference from adjacent antennas, interference rejection combining has been specified in the 4G Long-Term-Evolution (LTE) standard as a part of coordinated multi-point transmission, which consequently increases fronthaul traffic [8]. The amount of fronthaul traffic may be a significant problem though the same technologies can be used in the DAN. In this research, the DAS with joint maximum likelihood detection (MLD) is proposed for suppressing interference. Joint MLD treats the received signals as the superposition of the desired and the interference signals and regards them as a signal with a larger number of constellation points [9]–[11].

Scheduling the MTs to provide fairness and maintain good network throughput becomes the problem when there are more MTs in a network. In [12], the authors discuss three MT scheduling schemes, proportional-fair (PF), round-robin (RR), and max-carrier-to-interference (C/I), and their effects on downlink (DL) transmission in the DAS. It was concluded that RR scheduling achieves high fairness and throughput with a simple algorithm. MT scheduling in the DAS is also discussed in [13], where combining multiple scheduling algorithms to create a scheduling criteria achieved a fair and high throughput system.

The DAS with DAs that transmit on the DL to multiple MTs is assumed in this research. In the assumed DAS, it is

proposed that each MT demodulates signals for its own and the other via joint MLD and multi-MT scheduling is applied. For the multi-MT scheduling, RR scheduling is used with max-C/I as a selection algorithm for DAs. The proposed scheme is compared against the conventional scheme as well as a scheme without the use of joint MLD, where the throughput evaluation is based on the numerical analysis of multi-cell simulation using constellation constrained capacity (CCC).

This paper is organized as follows. Section 2 describes the system model and the conventional and proposed schemes. Section 3 presents numerical results obtained through computer simulation. Section 4 concludes this research.

II. System Model

A. Cell Model

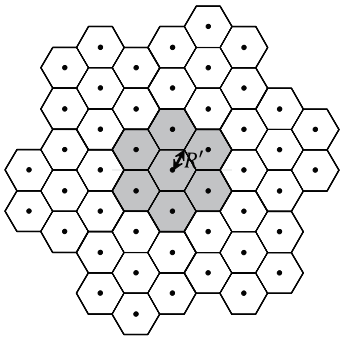

Fig. 2: DAS cell model ($N_{DA} = 7$).

A hexagonal-cell concept is assumed for the DAS cell model [14]. Each macro cell has uniformly distributed N_{DA} DAs. In this research, N_{DA} is set to seven. Each DA is placed in a smaller hexagonal-cell with a radius of R', as shown in Fig. 2. Surrounding the center cell, there are six other outer macro cells with the same configuration. Also, the center cell is assumed to be the cell of interest.

In the assumed DAS, the same channel is shared by the DAs in the cell. Also, the same frequency channel can be assigned to two DAs in each macro cell. In the receiver of a MT, joint MLD is applied to mitigate the CCI in the macro cell. The MT receives the signals transmitted from two DAs in the same macro cell. With the joint MLD, the receiver extracts its desired signal even though the signal for the other MT is transmitted from one of the other DAs on the same channel.

B. Scheduling

For the multiple MT scheduling, the RR scheduling of the MTs and the max-C/I scheduling (or selection) of the DAs are applied at the same time. For comparison, a single MT scheduling scheme is also considered in this research where each MT is chosen one at a time and the DA with the best C/I is chosen via the max-C/I scheduling. In the DAS, using all of the DAs in a dense cell can lead to CCI and, as reserached in [15], turning off some of the DAs in a multi-MT environment could increase transmission throughput. This is also the reason to reduce the number of receiving MTs to two per resource block (RB). Limiting the number of MTs lead to low CCI and improves system throughput with joint MLD.

Algorithm 1: Multi-MT scheduling algorithm.

Data: $\mathbf{P}$, N_{perm}, N_{frames}, N_{RB}, $\mathbf{H}^i_{f_\alpha}$, $\mathbf{H}^i_{f_\beta}$
begin
  $i = 1$
  for $f = 1 \rightarrow N_{frames}$ **do**
    $\bar{\mathbf{H}}^r_{f_\alpha} = \sum_{i \in \{i_r\}} \mathbf{H}^i_{f_\alpha}$
    $\bar{\mathbf{H}}^r_{f_\beta} = \sum_{i \in \{i_r\}} \mathbf{H}^i_{f_\beta}$
    for $r = 1 \rightarrow N_{RB}$ **do**
      $k_\alpha, k_\beta \leftarrow \mathbf{P}(i)$
1     $l^{max}_\alpha, l^{max}_\beta =$
        $\arg\max_{l_\alpha, l_\beta (l_\alpha \neq l_\beta)} (\bar{\mathbf{H}}^r_{f_\alpha}(k_\alpha, l_\alpha) + \bar{\mathbf{H}}^r_{f_\beta}(k_\beta, l_\beta))$
      $i = i + 1$
      if $i > N_{perm}$ **then**
        $i = 1$
      end
    end
  end
end

In detail, the proposed multi-MT scheduling algorithm is shown in Algorithm 1. The k_α-th and k_β-th MTs are chosen, and each MT receives its desired signal from the l_α-th and l_β-th DAs, respectively. N_{MT} represents the number of the MTs. N_{frame} and N_{RB} are the two resource factors, where N_{frame} represents the total number of frames and N_{RB} represents the total number of RBs. $\mathbf{P}$ defines all of the permutations of selecting two MTs out of the total N_{MT}, and the total number of permutations is given by $N_{perm} = {}_{N_{MT}}\mathrm{P}_2$ where ${}_n\mathrm{P}_r = \frac{n!}{(n-r)!}$. For example, the i-th index $\mathbf{P}(i)$ contains the scheduled MT pair, MT k_α and MT k_β, which means $(k_\alpha, k_\beta) \in \mathbf{P}$. Two MTs are selected per RB at each time index. $\mathbf{H}^i_{f_\alpha}$ and $\mathbf{H}^i_{f_\beta}$ are the channel matrix on the i-th subcarrier with a size of $N_{MT} \times N_{DA}$ and they are also assumed to be constant over N_{frames}. $\mathbf{H}^i_{f_\alpha}(k_\alpha, l_\alpha) = h^i_{k_\alpha, l_\alpha}$ and $\mathbf{H}^i_{f_\beta}(k_\beta, l_\beta) = h^i_{k_\beta, l_\beta}$ are the channel responses from the l_α-th and l_β-th DAs to the k_α-th and k_β-th MTs on the i-th subcarrier, respectively. In this algorithm, the DAs for each MT is chosen for the scheduled MTs, k_α and k_β, by finding the maximum sum of the channel responses, $\bar{\mathbf{H}}^r_{f_\alpha}(k_\alpha, l_\alpha) + \bar{\mathbf{H}}^r_{f_\beta}(k_\beta, l_\beta)$. As shown in line 1, the scheduled DAs are represented by l^{max}_α and l^{max}_β, and the total channel response for these pairs is $h^{i,max}_f = \bar{\mathbf{H}}^r_{f_\alpha}(k_\alpha, l^{max}_\alpha) + \bar{\mathbf{H}}^r_{f_\beta}(k_\beta, l^{max}_\beta)$.

C. Throughput Calculation

In this research, each MT is equipped with a single antenna and DL transmission is assumed. The system model for the

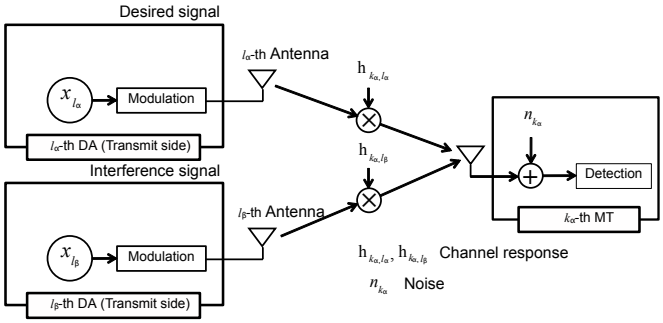

Fig. 3: System model for proposed scheme.

proposed scheme is shown in Fig. 3. In the assumed DAS, at most two DAs transmit at once on the same channel in the multi-MT scheduling. Each MT receives the desired signal as well as the interference signal from the other DA. Each MT also receives interference from the surrounding macro cells.

Suppose that $x^i_{l_\beta}(s^i_{l_\beta})$ is treated as an interference signal from the other l_β-th DA in the same cell and $s^i_{l_\beta}$ is the index for the constellation points of the interference signal on the i-th subcarrier. Also assume that $E[|x^i_{l_\alpha}(s^i_{l_\alpha})|^2] = [|x^i_{l_\beta}(s^i_{l_\beta})|^2] = 1$ and the number of constellation points of the interference signal is $N^i_{l_\beta}$ $(0 \le s^i_{l_\beta} \le N^i_{l_\beta} - 1)$. The received signal at the k_α-th MT, $y^i_{k_\alpha}$, on the i-th subcarrier is given as

$$\begin{aligned} y^i_{k_\alpha} &= h^i_{k_\alpha,l_\alpha} x^i_{l_\alpha}(s^i_{l_\alpha}) + h^i_{k_\alpha,l_\beta} x^i_{l_\beta}(s^i_{l_\beta}) \\ &+ \sum_{l'} h^i_{k_\alpha,l'} x^i_{l'}(s^i_{l'}) + n^i_{k_\alpha} \end{aligned} \quad (1)$$

and similarly, the k_β-th MT's received signal, $y^i_{k_\beta}$, is given as

$$\begin{aligned} y^i_{k_\beta} &= h^i_{k_\beta,l_\beta} x^i_{l_\beta}(s^i_{l_\beta}) + h^i_{k_\beta,l_\alpha} x^i_{l_\alpha}(s^i_{l_\alpha}) \\ &+ \sum_{l'} h^i_{k_\beta,l'} x^i_{l'}(s^i_{l'}) + n^i_{k_\beta}, \end{aligned} \quad (2)$$

where $h^i_{k,l}$ is the channel response from the l-th DA to the concerning k-th MT.

For throughput evaluation, the inter-cell interference is regarded as a Gaussian noise and is subject to Gaussian distribution. Therefore, Eqs. (1) and (2) can be rewritten as

$$y'^i_{k_\alpha} = h^i_{k_\alpha,l_\alpha} x^i_{l_\alpha}(s^i_{l_\alpha}) + h^i_{k_\alpha,l_\beta} x^i_{l_\beta}(k^i_{l_\beta}) + z^i_{k_\alpha}, \quad (3)$$

$$y'^i_{k_\beta} = h^i_{k_\beta,l_\beta} x^i_{l_\beta}(s^i_{l_\beta}) + h^i_{k_\beta,l_\alpha} x^i_{l_\alpha}(k^i_{l_\alpha}) + z^i_{k_\beta}, \quad (4)$$

where z^i_k is the sum of the inter-cell interference and the additive white Gaussian noise (AWGN) with the variance of σ^2.

Two demodulation schemes for MLD are researched in this paper. In the first scheme, system throughput when the MT applies MLD for the desired signal only is calculated. In this case, the signal for the other MT in the same cell is treated as CCI. From Eqs. (3) and (4), the CCC with the MLD is given as Eqs. (5) and (6) [9], [16]. The system throughput is then calculated by the sum of the entire RB given by,

$$T_m = \sum_i \left[\sum_{r=1}^{N_{RB}} T_m{}^r_{k_\alpha r} + \sum_{r=1}^{N_{RB}} T_m{}^r_{k_\beta r} \right]. \quad (7)$$

On the other hand, the throughput of the joint MLD scheme is also calculated. In this case, the receiver of the MT jointly demodulates the signals for the concerning MT and another one in the same cell. The CCC with the joint MLD is given as Eqs. (8) and (9). The system throughput is then calculated by

$$T_j = \sum_i \left[\sum_{r=1}^{N_{RB}} T_j{}^r_{k_\alpha r} + \sum_{r=1}^{N_{RB}} T_j{}^r_{k_\beta r} \right]. \quad (10)$$

As for the single-MT scheduling, a single MT in each macro cell is scheduled for a particular frame's RB. Therefore, MLD is applied. The system throughput is calculated by taking only the k^r-th MT in Eq. (7), which is given by,

$$T = \sum_i \sum_{r=1}^{N_{RB}} T^r_{k^r}. \quad (11)$$

III. Numerical Results

A. Simulation Conditions

Multi-cell system-level simulation is conducted to compare the system throughputs of the conventional schemes, the single-MT scheduling, the multi-MT scheduling with MLD, and the proposed multi-MT scheduling with joint MLD scheme. Simulation conditions are presented in Table I. A seven hexagonal macro-cell model with a seven hexagonal DA cell in each macro-cell is assumed as shown in Fig. 2. The inter-antenna distance between adjacent DAs is changed from 25 m to 250 m. N_{MT} MTs are dropped randomly with an uniform distribution and they are dropped farther than 5 m from DAs. Distance dependent path loss with a decay factor of 36.7 and log-normal shadowing with standard deviation of 8 dB is used for the propagation model. The shadowing correlation between the antennas are set to 0.5. A one-path Rician fading channel model with a $\mathcal{K}$-factor of 10 is assumed for the cell of interest and a six-path Rayleigh fading channel model is assumed for the macro-cells surrounding the cell of interest. For comparison of different channels, a six-path Rayleigh fading channel model is also used for the cell of interest. The system bandwidth is set to 4.32 MHz. The number of RBs, N_{RB}, is 24 and the number of subcarriers for each RB is 12. The symbols are modulated with QPSK, 16QAM, 64QAM, or 256QAM on each subcarrier. Each DA has a height of 10 m and the transmit power is 30 dB. Each MT is set at a height of 1.5 m and the receiver noise density is -174 dBm/Hz. The throughputs in Eqs. (7), (10), and (11) of the conventional and proposed schemes are simulated through

$$T_{m^i_{k_\alpha}} = \log_2(N^i_{l_\alpha}) - \frac{1}{N^i_{l_\alpha} N^i_{l_\beta}} \sum_{s^i_{l_\alpha}=0}^{N^i_{l_\alpha}-1} \sum_{s^i_{l_\beta}=0}^{N^i_{l_\beta}-1} \underset{z^i_{k_\alpha}}{E} \left[\log_2 \frac{\sum_{t^i_{l_\alpha}=0}^{N^i_{l_\alpha}-1} \exp(-|h^i_{k_\alpha,l_\alpha}\{x^i_{l_\alpha}(s^i_{l_\alpha}) - x^i_{l_\alpha}(t^i_{l_\alpha})\} + h^i_{k_\alpha,l_\beta} x^i_{l_\beta}(s^i_{l_\beta}) + z^i_{k_\alpha}|^2/\sigma^2)}{\exp(-|h^i_{k_\alpha,l_\beta} x^i_{l_\beta}(s^i_{l_\beta}) + z^i_{k_\alpha}|^2/\sigma^2)} \right] \tag{5}$$

$$T_{m^i_{k_\beta}} = \log_2(N^i_{l_\beta}) - \frac{1}{N^i_{l_\beta} N^i_{l_\alpha}} \sum_{s^i_{l_\beta}=0}^{N^i_{l_\beta}-1} \sum_{s^i_{l_\alpha}=0}^{N^i_{l_\alpha}-1} \underset{z^i_{k_\beta}}{E} \left[\log_2 \frac{\sum_{t^i_{l_\beta}=0}^{N^i_{l_\beta}-1} \exp(-|h^i_{k_\beta,l_\beta}\{x^i_{l_\beta}(s^i_{l_\beta}) - x^i_{l_\beta}(t^i_{l_\beta})\} + h^i_{k_\beta,l_\alpha} x^i_{l_\alpha}(s^i_{l_\alpha}) + z^i_{k_\beta}|^2/\sigma^2)}{\exp(-|h^i_{k_\beta,l_\alpha} x^i_{l_\alpha}(s^i_{l_\alpha}) + z^i_{k_\beta}|^2/\sigma^2)} \right] \tag{6}$$

$$T_{j^i_{k_\alpha}} = \log_2(N^i_{l_\alpha}) - \frac{1}{N^i_{l_\alpha} N^i_{l_\beta}} \sum_{s^i_{l_\alpha}=0}^{N^i_{l_\alpha}-1} \sum_{s^i_{l_\beta}=0}^{N^i_{l_\beta}-1} \underset{z^i_{k_\alpha}}{E} \left[\log_2 \frac{\sum_{t^i_{l_\alpha}=0}^{N^i_{l_\alpha}-1} \sum_{t^i_{l_\beta}=0}^{N^i_{l_\beta}-1} \exp(-|h^i_{k_\alpha,l_\alpha}\{x^i_{l_\alpha}(s^i_{l_\alpha}) - x^i_{l_\alpha}(t^i_{l_\alpha})\} + h^i_{k_\alpha,l_\beta}\{x^i_{l_\beta}(s^i_{l_\beta}) - x^i_{l_\beta}(t^i_{l_\beta})\} + z^i_{k_\alpha}|^2/\sigma^2)}{\sum_{t^i_{l_\beta}=0}^{N^i_{l_\beta}-1} \exp(-|h^i_{k_\alpha,l_\alpha}\{x^i_{l_\beta}(s^i_{l_\beta}) - x^i_{l_\beta}(t^i_{l_\beta})\} + z^i_{k_\alpha}|^2/\sigma^2)} \right] \tag{8}$$

$$T_{j^i_{k_\beta}} = \log_2(N^i_{l_\beta}) - \frac{1}{N^i_{l_\beta} N^i_{l_\alpha}} \sum_{s^i_{l_\beta}=0}^{N^i_{l_\beta}-1} \sum_{s^i_{l_\alpha}=0}^{N^i_{l_\alpha}-1} \underset{z^i_{k_\beta}}{E} \left[\log_2 \frac{\sum_{t^i_{l_\beta}=0}^{N^i_{l_\beta}-1} \sum_{t^i_{l_\alpha}=0}^{N^i_{l_\alpha}-1} \exp(-|h^i_{k_\beta,l_\beta}\{x^i_{l_\beta}(s^i_{l_\beta}) - x^i_{l_\beta}(t^i_{l_\beta})\} + h^i_{k_\beta,l_\alpha}\{x^i_{l_\alpha}(s^i_{l_\alpha}) - x^i_{l_\alpha}(t^i_{l_\alpha})\} + z^i_{k_\beta}|^2/\sigma^2)}{\sum_{t^i_{l_\alpha}=0}^{N^i_{l_\alpha}-1} \exp(-|h^i_{k_\beta,l_\beta}\{x^i_{l_\alpha}(s^i_{l_\alpha}) - x^i_{l_\alpha}(t^i_{l_\alpha})\} + z^i_{k_\beta}|^2/\sigma^2)} \right] \tag{9}$$

TABLE I: Simulation conditions.

Cell layout	7 DA system
Inter-antenna distance	25, 50, 100, 150, 200, 250 m
Minimum distance between MT and DA	5 m
Path loss	$140.7 + 36.7 \log_{10}(R)$ dB, R: Distance [km]
Height of antennas	10 m
Height of MTs	1.5 m
Shadowing deviation	8 dB
Shadowing correlation	0.5
Channel model (inner)	One-path Rician ($\mathcal{K}$ = 10) Six-path Rayleigh
Channel model (outer)	Six-path Rayleigh
Number of MTs	5, 7, 10, 15, 20, 25
Transmit power	30 dBm
Receiver noise density	-174 dBm/Hz
System bandwidth	4.32 MHz
RB bandwidth	180 kHz
Number of RBs	24
Modulation scheme	QPSK, 16QAM, 64QAM, 256QAM
MT drops	200
Trials per MT drop	5
Number of symbols per trial	100

Monte Calro simulation [16]. The number of MT drops is 200 and the number of trials per MT drop is five. The channel response is renewed for each trial. The number of transmit symbols for each trial is 100.

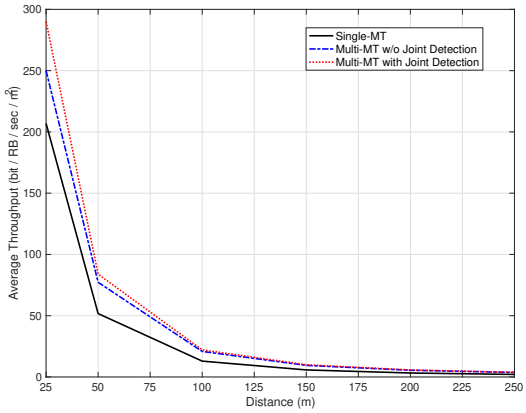

Fig. 4: Average throughput per area versus inter-DA distance.

B. Throughput Characteristics

Figure 4 presents the average throughput per area versus the inter-DA distance of the DAs. The number of MTs are set to seven. The effect of joint MLD can be seen greatly according to the inter-antenna distance of the DAs. As shown in Fig. 4, when the distance between the DAs are longer, such as from 150 to 250 m, the throughput differences among those schemes diminish. On the other hand, if the distances between adjacent DAs is shorter, such as from 25 to 50 m, the throughput differences are greater. By comparing the single and multi-MT schemes, in the shorter inter-DA distance DAS, the multi-MT schemes provide better system throughput. In the multi-MT schemes, when the inter-antenna distance is 25 m, the throughput with joint MLD is higher than the one without joint MLD, whereas in the other distances, the multi-MT scheduling with and without joint MLD achieves the same improvements. This is due to the fact that in the shorter inter-DA distance

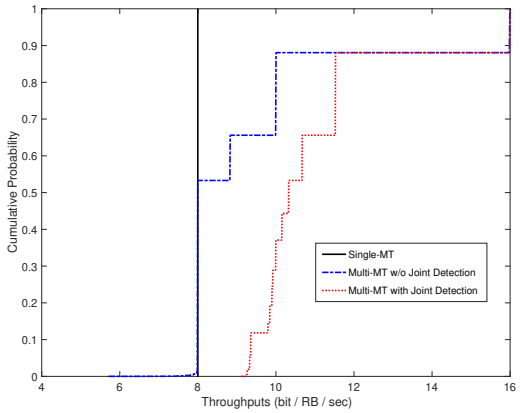

Fig. 5: CDF for inter-DA distance of 25 m.

DAS, the channel is more likely to be interfered by the signals from the surrounding DAs than that when the cells were more widely spread out. Joint MLD provides better throughput since this scheme mitigates the effect of the interference.

In Fig. 5, the cumulative distribution function (CDF) curves of the system throughput for inter-DA distance of 25 m is presented. In the figure, single-MT scheme only transmits around 8 bits / RB / sec since only one MT is allowed to transmit at a specific resource slot. At a particular resource slot, the assigned MT is not affected by CCI since interference will come only from the outer macro cells, which is assumed to be farther than the connected antenna. This means that these MTs can transmit symbols with higher order modulation, such as 256QAM. On the other hand, in the multi-MT schemes, at most, two MTs can transmit for each resource slot. If two MTs can transmit at 256QAM, the throughput will be 16 bits / RB / sec. As clearly shown in the figure, around half of the resource slots in the multi-MT scheme without joint MLD can transmit at 8 bits / RB / sec, whereas the scheme with joint MLD provides the MTs that transmit at greater throughput which means that those resource slots can now transmit two MTs at once. This shows how joint MLD can provide better system throughput when the DAs are closer to one another. In Fig. 5, around 87% of the MTs are able to transmit at throughput of 9.7 bits / RB /sec without joint MLD, whereas 87% of the MTs are able to transmit at throughput of 11.6 bits / RB / sec. Joint MLD enables the simultaneous transmission of all of the MTs in each resource slot.

IV. Conclusions

In this research, the DAS with joint MLD has been proposed by taking in consideration of scheduling the multiple MTs. The system throughout for the proposed scheme has been compared with those of the conventional single-MT scheduling and the multi-MT scheduling without the joint MLD in system level simulation. As a result, using joint MLD in the multi-MT scheduling scheme increases system throughput. Especially, when the inter-DA distance is 25 m, the system throughput improved around 15%.

Acknowledgments

This work is supported in part by a Grant-in-Aid for Scientific Research (C) under Grant No.16K06366 from the Ministry of Education, Culture, Sport, Science, and Technology in Japan.

References

[1] *DOCOMO 5G White Paper*, NTT DOCOMO, INC., July 2014.
[2] *Mobile Communications System for 2020 and Beyond White Paper*, ARIB 2020 and Beyond Ad Hoc Group, Oct. 2014.
[3] F. Adachi, W. Peng, T. Obara, T. Yamamoto. R. Matsukawa, and M. Nakada, "Distributed Antenna Network for Gigabit Wireless Access," 54th IEEE International Midwest Symposium on Circuits and Systems, Aug. 2011.
[4] A. A. M. Saleh, A. J. Rustako, and R. S. Roman, "Distributed Antennas for Indoor Radio Communications," IEEE Trans. on Commun., vol. 35, no.12, pp. 1245-1251, Dec. 1987.
[5] W. Choi, and J. G. Andrews, "Downlink Performance and Capacity of Distributed Antenna Systems in a Multicell Environment," IEEE Trans. on Commun., vol. 6, no. 1, pp. 69-73, Jan. 2007.
[6] H. Kaji, S. Kumagai, K. Temma, and F. Adachi, "Spectrum-Energy Efficiency Tradeoff of Distributed Antenna Network," IEEE 11th Vehicular Technology Society Asia Pacific Wireless Communications Symposium, Aug. 2014.
[7] S. Kumagai, R. Matsukawa, T. Obara, T. Yamamoto, and F. Adachi, "Spectral Efficiency of Distributed Antenna Network Using MIMO Spatial Multiplexing," IEEE 76th Veh. Technol. Conf., Sept. 2012.
[8] T. Abe, Y. Kishiyama, Y. Kakura, and D. Imamura, "Radio Interface Technologies for Cooperative Transmission in 3GPP LTE-Advanced," IEICE Trans. on Comun., vol. E94-B, no. 12, Dec. 2011.
[9] T. Yazaki and Y. Sanada, "Effect of Joint Detection in Far User on Non-orthogonal Multiple Access Downlink," Wireless Pers. Commun., vol. 86, pp. 1203-1219, Aug. 2016.
[10] T. Yazaki and Y. Sanada, "Throughput Performance of Non-orthogonal Multiple Access with Joint Detection in Far User," International Symposium on Intelligent Signal Processing and Communication Systems, Nov. 2015.
[11] H. Miyagi and Y. Sanada, "MMSE Interference Rejection Followed by Joint Maximum Likelihood Detection for Distributed Antenna Network," 23rd Asia-Pacific Conf. on Commun., Dec. 2017.
[12] Y. Seki and F. Adachi, "Downlink Capacity Comparison of MMSE-SVD and BD-SVD for Cooperative Distributed Antenna Transmission using Multi-user Scheduling," IEEE 86th Veh. Technol. Conf., Sept. 2017.
[13] Y. Xin, R. Zhang, D. Wang, J. Li, L. Yang, X. You, "Antenna Clustering for Bidirectional Dynamic Network With Large-Scale Distributed Antenna Systems," IEEE Access, vol. 5, pp. 4037-4047, Feb. 2017.
[14] V.H. Mac Donald, "Advanced Mobile Phone Service: The Cellular Concept," Bell Syst. Tech., vol. 58, no. 1, Jan. 1979.
[15] H. Tabassum, U. Siddique, E. Hossain, J. Hossain, "Downlink Performance of Cellular Systems With Base Station Sleeping, User Association, and Scheduling," IEEE Trans. on Commun., vol. 13, issue 10, pp. 5752-5767, July 2014.
[16] G. Ungerboeck, "Channel Coding with Multilevel/Phase Signals," IEEE Trans. on Info. Theory, vol. IT-28, no. 1, pp. 55-67, Jan. 1982.